

Thermally Stable Cross-linked P84 with Superior Membrane H₂/CO₂ Separation Properties at
100 °C

Maryam Omidvar¹, Christopher M. Stafford², and Haiqing Lin^{1,*}

¹Department of Chemical and Biological Engineering, University at Buffalo, The State University of New York, Buffalo, Buffalo, NY 14260, USA

²Materials Science & Engineering Division, National Institute of Standards and Technology, MS 8542, 100 Bureau Drive, Gaithersburg, MD 20899, USA

* Corresponding author. Tel: +1-716-645-1856, Email: haiqingl@buffalo.edu (H. Lin)

Prepared for submission to *Journal of Membrane Science*

November 14, 2018

Abstract

Polymers with a strong size-sieving ability and superior H₂/CO₂ selectivity are of great interests for pre-combustion CO₂ capture at 100 °C or above. Polyimides (such as Matrimid[®] and 6FDA-durene) have been cross-linked using diamines and show superior H₂/CO₂ selectivity. However, these cross-linked polymers cannot be used for the pre-combustion CO₂ capture because of the lack of thermal stability at 100 °C. Herein we demonstrate that commercial P84[™] can be chemically cross-linked using 1,4-butanediamine (BuDA) to achieve robust H₂/CO₂ separation properties at 100 °C to 150 °C. The cross-linked P84 were thoroughly evaluated using Fourier transform infrared spectroscopy (FTIR), X-ray photoelectron spectroscopy (XPS), differential scanning calorimetry (DSC), and thermogravimetric analysis (TGA). The effects of the cross-linking time on the physical properties and H₂/CO₂ separation properties at various temperatures were determined and interpreted using a free volume model. An exemplary sample based on P84 crosslinked by BuDA for 6 h exhibits a H₂ permeability of 47 Barrers (1 Barrer = 3.35×10^{-16} mol m/m²·s·Pa) and H₂/CO₂ selectivity of 14 at 100 °C, which is on the Robeson's upper bound, indicating their potential for practical applications.

Keywords: P84; Cross-linking; Membranes; H₂/CO₂ separation; Diamine

1. Introduction

Membrane technology has attracted significant interests for H₂ purification and CO₂ capture in pre-combustion processes because of its inherently high energy-efficiency [1-4]. Particularly, membrane materials with high H₂ permeability and H₂/CO₂ selectivity at the syngas processing temperatures such as 100 °C or above provide a low-cost route for the CO₂ capture [5-7]. For example, membranes with a H₂/CO₂ selectivity of 10 at 150 °C were shown to achieve 90% CO₂ capture from the pre-combustion processes at an energy consumption 32% less than the current leading technology of Selexol absorption [5].

Glassy polymers have been explored for H₂/CO₂ separation at high temperatures because of their strong size-sieving ability and thus high H₂/CO₂ diffusivity selectivity [8], such as polybenzimidazole (PBI) [7, 9], cross-linked PBI [3, 10], and highly cross-linked polyamides [11]. Conventional polyimides do not have sufficiently high H₂/CO₂ selectivity despite their huge design space of diamines and dianhydrides, low cost, and significant know-how in preparing hollow fiber membranes, partially because of the insufficient size-sieving ability. For example, typical polyimides of Matrimid[®] 5218 and 6FDA-durene (where 6FDA and durene are 4,4'-(hexafluoroisopropylidene) diphthalic anhydride and 2,3,5,6-tetramethyl-1,4-phenylenediamine, respectively) show a H₂/CO₂ selectivity of only 3.7 and 1.0 at 35 °C, respectively [12, 13].

Cross-linking polyimides using diamines is a convenient way to dramatically enhance the H₂/CO₂ selectivity [6, 14-23], in large part due to the increase in size-sieving ability. For example, the cross-linking of 6FDA-durene using 1,4-butanediamine (BuDA) for 10 min increases the H₂/CO₂ selectivity from 1.0 to 102 at 35 °C [12, 16, 18, 23], and the cross-linking of 6FDA-ODA/NDA (where ODA and NDA are 4,4'-oxydianiline and 1,5-naphthalenediamine, respectively) using 1,3-diaminopropane (PDA) for 2 h increases the H₂/CO₂ selectivity from 2.3 to 60 at 35 °C

[17, 24]. Hollow fiber membranes based on 6FDA-NDA (NDA=1,5-diamino naphthalene), PBI/Matrimid blends, and Torlon were prepared and cross-linked using ethylenediamine (EDA) vapor [25]. After 5 min reaction, the 6FDA-NDA membranes showed a H₂ permeance of 3.4 GPU (1 GPU = 10⁻⁶ cm³(STP)/cm² s cmHg) and a H₂/CO₂ selectivity of 35 at 35 °C [25]. However, the cross-linked Matrimid, 6FDA-durene, and 6FDA-ODA (ODA = 4,4'-diamino diphenyl ether) are not stable at temperatures above 100 °C, where the crosslinking reaction reverses to produce imide rings and release the diamines [14, 15, 17, 26, 27]. Therefore, these materials are not suitable for the pre-combustion CO₂ capture (preferred to be at 100 °C or above). Moreover, from a fundamental perspective, the cross-linking reaction was performed with thick films (50 μm), and the reaction only occurs on the surface and not in bulk (as indicated by the low gel content in the cross-linked samples) [16-18, 23, 24]. Therefore, there lacks a fundamental understanding of the effect of cross-linking on the H₂/CO₂ separation properties in polyimides.

P84TM is a commercially available polyimide with a strong size-sieving ability and higher pure-gas H₂/CO₂ selectivity (5.3) than Matrimid (3.7) or 6FDA-durene (1.0) at 35 °C [22]. P84 had been prepared into flat-sheet membranes for organic solvent nanofiltration [28, 29] and hollow fiber membranes for pervaporation and CO₂/CH₄ separation [30, 31]. Asymmetric hollow fiber membranes based on P84 were also cross-linked with 1,5-diamino-2-methylpentane (DAMP), which increased the H₂/CO₂ selectivity from 5.3 to 16 at 35 °C [22]. However, no studies on the cross-linked P84 for H₂/CO₂ separation at elevated temperatures are available in the literature.

In this study, we systematically investigate the effect of the bulk cross-linking of P84 using diamines on H₂/CO₂ separation at temperatures ranging from 35 °C to 150 °C. Freestanding 15-μm thick films were fully cross-linked and demonstrated to be stable at temperatures up to 150 °C. The effect of the cross-linking time and agents such as BuDA, p-xylene diamine (XDA), and PDA

on the polymer properties were determined. The H₂/CO₂ separation properties at 100 °C and 150 °C are compared with the literature data in the Robeson's upper bound plots to demonstrate that the cross-linking of P84 can be a useful way to achieve superior H₂/CO₂ separation properties at temperatures relevant to the pre-combustion CO₂ capture.

2. Experimental

2.1. Materials

Equipment and instruments or materials are identified herein to adequately specify the experimental details. Such identification does not imply recommendation by the National Institute of Standards and Technology, nor does it imply the materials are necessarily the best available for the purpose.

P84 was purchased from HP Polymer Inc. (Lenzing, Austria). Methanol, BuDA, PDA, and XDA were supplied by Sigma-Aldrich Corporation (St. Louis, MO, USA). N-methyl-2-pyrrolidone (NMP) was purchased from Fisher Scientific International, Inc. (Hampton, NH, USA). Novec 7300 engineered fluid (1,1,1,2,2,3,4,5,5,5-decafluoro-3-methoxy-4-(trifluoromethyl)-pentane) was obtained from 3M Company (St. Paul, MN, USA). Gas cylinders of H₂ and CO₂ with ultrahigh purity were obtained from Jackson Welding & Gas Products (Buffalo, NY, USA).

2.2. Preparation of the cross-linked P84 films

To prepare freestanding films, P84 was first dissolved in NMP at 10 % by mass. After mixing, the homogeneous solution was filtered using a filter with a pore size of 1.0 μm. The solution was then cast on a glass plate and allowed to dry in a fume hood. Finally, the film was dried in a conventional oven at 80 °C for 15 h and then in a vacuum oven at 200 °C for 48 h to remove the residual NMP (with a boiling temperature of 203 °C). The obtained film has a thickness

of $15 \mu\text{m} \pm 2 \mu\text{m}$.

Freestanding films of P84 were cross-linked by immersing in methanol containing 1 mol/L BuDA for a desired period. The films were then washed with fresh methanol for 3 times and then dried at 80 °C for 24 h to remove the methanol. The cross-linked samples were labeled as XLP84-*t*h (where *t* represents the cross-linking time in hours).

2.3. Characterization of chemical and physical properties of XLP84

The changes in the chemical structure of P84 after cross-linking were monitored by Attenuated total reflection Fourier transform infrared (ATR FTIR) spectroscopy (Vertex 70, Bruker, MA) with a resolution of 4 cm^{-1} .

Glass transition temperature (T_g) of P84 and XLP84 was determined using differential scanning calorimetry (DSC, Q2000, TA Instruments, DE). The measurement was performed at a heating rate of 10 °C/min from 25 °C to 400 °C under a nitrogen flow of 50 mL/min. The T_g value was taken as the midpoint of the heat capacity step change using the Universal Analysis software (TA instrument).

Thermal stability of P84 and XLP84 was determined using a thermogravimetric analyzer (TGA, Netzsch TG 209 F1, Germany). The measurement was performed with a ramping rate of 10 °C/min from 25 °C to 800 °C under a nitrogen flow of 100 mL/min.

X-ray photoelectron spectroscopy (XPS) was used for elemental analysis of the polymer films. XPS measurements were performed using a Kratos AXIS Ultra DLD Spectrometer (Kratos Analytical, Manchester, UK) with a monochromatic Al K_{α} source (1486.6 eV) operating at 140 W. The base pressure of the sample analysis chamber was $\approx 1.0 \times 10^{-9}$ Torr (or 1.33×10^{-7} Pa), and spectra were collected from a nominal spot size of $300 \mu\text{m} \times 700 \mu\text{m}$. Measurements were

performed in hybrid mode using electrostatic and magnetic lenses, and the pass energy of the analyzer was set at 160 eV for survey scans and 20 eV for high resolution scans, with energy resolutions of 0.5 eV and 0.1 eV. All XPS data analysis was performed using the CasaXPS software package.

The gel content of the XLP84 was measured by immersing the film (with a mass of m_1) in NMP for 24 h. The insoluble material was dried at 200 °C for 24 h and then weighted with a mass of m_{gel} . The gel content (w_{gel}) was calculated using eqn (1):

$$w_{gel} = \frac{m_{gel}}{m_1} \times 100\% \quad (1)$$

The density of the polymer films was determined using Archimedes' principle and an analytical balance (Model XS64, Mettler-Toledo, OH) equipped with a density kit at 21 °C [32]. Novec 7300 engineered fluid was used as an auxiliary liquid because the solvent has low sorption in the polymers. The liquid has a density of 1.66 g/cm³ at 21 °C.

Fractional free volume (*FFV*) is an important factor determining gas diffusivity, which can be calculated using eqn (2):

$$FFV = \frac{V - 1.3V_w}{V} \quad (2)$$

where V is the specific volume of the polymer and V_w is the van der Waals volume, which can be estimated by a group contribution method [33]. For the XLP84 samples, the V_w value was calculated by considering the gel composition (or the molar ratio of the reacted BuDA and P84 repeating units, as shown in eqn (4)).

2.4. Determination of gas permeation and sorption

Pure-gas permeation measurement was performed using a constant-volume/variable-pressure apparatus at 35 °C to 150 °C [34]. The polymer film was first masked using a brass disc

and high-temperature epoxy adhesive and then installed in a permeation cell in an oven with controlled temperatures. Gas permeability (P_A) was determined by monitoring a steady-state pressure increase in the volume on the permeate side of the film. The P_A has a unit of Barrers, where 1 Barrer = 10^{-10} cm³ (STP) cm/(cm² s cmHg). The obtained permeability values have an uncertainty of $\approx 10\%$, which can be estimated using a standard propagation of error analysis [35].

Gas solubility in polymers was determined using a microbalance (IGA 001, Hiden Isochema, Warrington, UK) at 35 °C to 150 °C [10, 32]. Polymer samples with ~ 70 mg were used, and the gas pressure was varied from 0.1 atm to 12 atm. Gas sorption at each pressure was considered at equilibrium when the microbalance reading remained unchanged for more than 1 h. The gas sorption is calculated using the mass change of the polymer samples considering the buoyancy effect [32]. The uncertainty of the gas solubility is estimated to be $\approx 5\%$ using the standard propagation of error analysis [35].

3. Results and discussion

3.1. Reaction of P84 and BuDA

Because the cross-linking of P84 occurs in methanol, the sorption kinetic of methanol in the P84 freestanding films were investigated. Fig. 1 illustrates the two-stage kinetic of methanol sorption in the P84 films including the Fickian diffusion and structural relaxation. In the first stage (first 6 h), methanol diffuses in the polymer following the Fickian diffusion mechanism. In the second stage (after 6 h), the polymer chains swell, and the structure rearranges because of the methanol plasticization, which further increases the methanol sorption and differs from the Fickian diffusion. Such two-stage kinetics has been reported for the sorption of organic vapor in glassy polymers [36]. After the sorption experiments, the P84 films were dried at 80 °C and showed the weight

almost the same as that before the sorption experiments, confirming that P84 has negligible solubility in methanol.

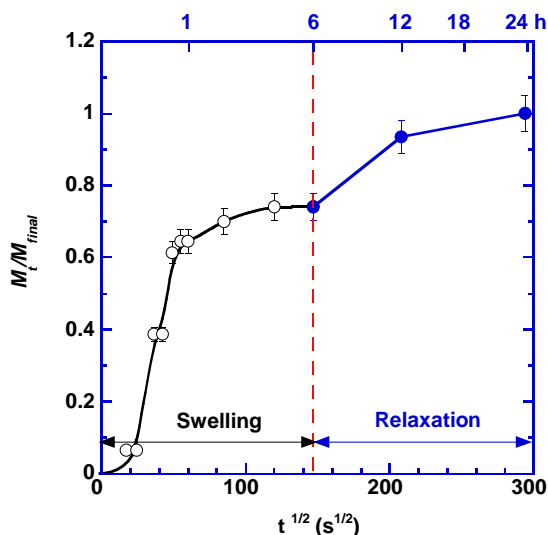


Fig. 1. The two-stage kinetics of methanol uptake in 15- μm thick P84 films at 21 °C. M_t is the mass of methanol sorbed by the P84 at an immersion time of t , and M_{final} is the equilibrium mass uptake of methanol (0.050 g methanol/g P84). The error bars represent one standard deviation of the data, which is taken as the experimental uncertainty of the measurement.

Fig. 2 shows the possible reactions between P84 and BuDA including grafting, cross-linking, and chain scission [13, 17, 22]. As one of the amine groups in the BuDA reacts with an imide ring on the backbone of the P84, the imide ring opens, grafting the BuDA and forming two amide groups. If the other amine group of the BuDA reacts with another P84 chain, cross-linking occurs. The electrophilic amide groups are susceptible to nucleophilic attacks, and therefore, they can exchange with the amine groups partially because the BuDA is excessive in the methanol solution. Consequently, if one imide group reacts with two BuDA modules, chain scission occurs, resulting in short P84 chains (or sol) that may be soluble in methanol [17].

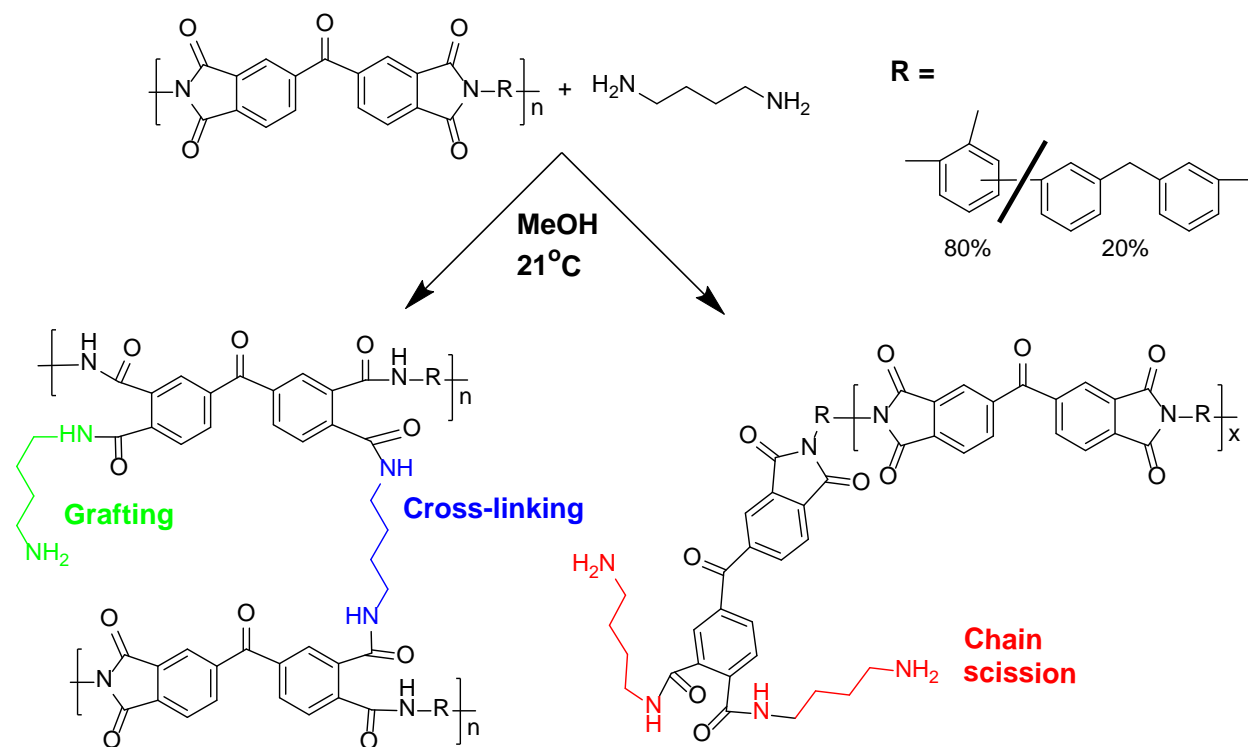


Fig. 2. Possible reaction mechanisms of P84 and BuDA in methanol at 21 °C including grafting, cross-linking, and chain scission.

Fig. 3 compares the FTIR spectra of P84 and two cross-linked P84 samples (XLP84-6h and XLP84-12h). Both XLP84-6h and XLP84-12h exhibit two characteristic amide peaks of 1654 cm^{-1} (C=O stretching) and 1534 cm^{-1} (C-N stretching) [29, 31, 37], which are not presented in the P84 spectrum. On the other hand, all samples show the characteristic imide peaks of 1780 cm^{-1} (C=O asymmetric stretching), 1715 cm^{-1} (C=O symmetric stretching), and 1356 cm^{-1} (C-N stretching) [29, 31, 37], suggesting that not all the imide groups are converted to the amides after the cross-linking. The imide groups are important to retain the long polymer chains or cross-linked structure.

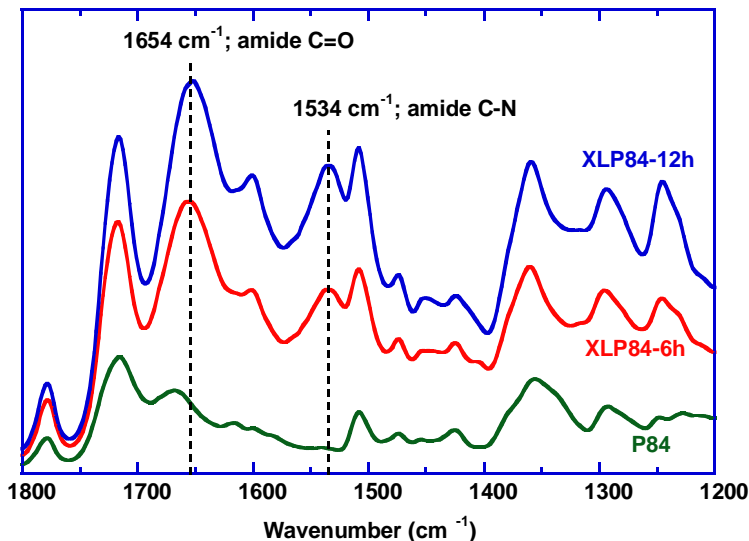


Fig. 3. Comparison of FTIR spectra of P84 and XLP84 samples confirming the reaction between P84 and BuDA. The peaks are not normalized.

Table 1 records the physical and chemical properties of the XLP84 samples. After the cross-linking, the samples were dried in the air and then in an oven at 80 °C to remove the residue methanol. The mass change is defined as the percentage of the mass increase after the cross-linking relative to the pristine P84 film. Surprisingly, the immersion of the P84 films in the BuDA solutions decreases the mass, which is caused by the chain scission (cf. Fig. 2), generating small P84 chains that are soluble in methanol. For example, the XLP84-6h shows a mass loss of 2.6 % compared with the pristine P84 film, though the solubility of P84 is negligible in methanol. As a comparison, Matrimid films exhibited a mass gain of 16 % under the same cross-linking condition in the methanol solution, which is also consistent with the literature study [13].

Table 1.

Chemical and physical properties of XLP84 samples, including weight change, gel content, density, T_g , elemental information, the molar ratio of BuDA to the P84 repeating units (r), estimated BuDA content, and FFV .

Sample	Weight change (%)	w_{gel} (%)	Density (g/cm ³)	T_g (°C)	O content (mol%)	N content (mol%)	r	BuDA content (% by mass)	FFV
P84	-	0	1.351±0.005	326±1	14.2	5.2	0	0	0.136±0.003
XLP84-1h	-2.1±0.2	95±1	1.363±0.005	324±1	11.5	8.8	0.57	11	0.114±0.003
XLP84-6h	-2.6±0.2	95±1	1.386±0.005	317±1	11.4	10	0.87	15	0.091±0.003
XLP84-12h	-2.9±0.2	96±1	1.367±0.005	315±1	11.4	9.3	0.69	13	0.107±0.003
XLP84-24h	-3.4±0.2	98±1	1.336±0.005	320±1	11.1	9.9	0.84	15	0.126±0.003
XLMatrimid-6h	16±1						0.68	14	

Table 1 also shows the gel content of the XLP84 samples. After 1 h immersion in the BuDA solution, the film shows the gel content as high as 95 %, indicating an almost complete cross-linking of the P84 chains. Further increase in the cross-linking time only slightly increases the gel content, indicating that the center of the bulk film is also fully cross-linked after 1 h cross-linking. This result is different from the literature, where the films were cross-linked for much shorter time (≈ 10 min), and the surface had much higher cross-linking density than the center of the films [17, 20].

As the cross-linking time increases, the T_g of XLP84 decreases before increasing, which can be ascribed to the opposite effect of the copolymer effect from the flexible BuDA and the enhanced chain rigidity from the highly cross-linking network [19, 38, 39]. On the other hand, the density increases before decreasing with increasing the cross-linking time. Initially, increasing the cross-linking time tightens the polymer structure and thus increases the density, while the further increase in the cross-linking time increases the BuDA content and causes the structural relaxation of the polymer chains in the methanol (as shown in Fig. 1) [10, 17], both decreasing the density.

Table 1 also presents the effect of cross-linking on the elemental information of the surface (<10 nm depth) derived from the XPS results. P84 shows an O content of 14.2 mol% and N content of 5.2 mol%, which are very close to the theoretical values (*i.e.*, O content of 15.5 mol% and N content of 6.2 mol%). In general, the exposure of P84 films with BuDA decreases the O content and increases the N content, confirming the generation of the amide groups in the XLP84 samples (as shown in Fig. 2).

The N content (x_N) can be used to calculate the mass ratio of the BuDA and P84 (m_B/m_{P84}) based on the mass balance with the following equation:

$$\frac{2m_B}{M_{w,B}} + \frac{2m_{P84}}{M_{w,P84}} = x_N \left(\frac{6m_B}{M_{w,B}} + \frac{32m_{P84}}{M_{w,P84}} \right) \quad (3)$$

where $M_{w,P84}$ (360 g mol⁻¹) and $M_{w,B}$ (88 g mol⁻¹) is the molecular mass of a P84 repeating unit and BuDA, respectively. BuDA has two N atoms out of 6 atoms of C and N , while a typical P84 repeating unit has two N atoms out of 32 atoms of C , N , and O .

The molar ratio of the BuDA to P84 repeating units (r) is calculated using the following equation:

$$r = \frac{m_B}{m_{P84}} \times \frac{M_{w,P84}}{M_{w,B}} \quad (4)$$

The 1 h cross-linking leads to an r value of 0.57, consistent with the gel content of 95%. As the cross-linking time increases, the r value increases due to the increased grafting reaction or even chain scission, as shown in Fig. 2. Table 1 also shows the estimated BuDA content in the XLP84 (*i.e.*, $m_B/(m_B + m_{P84})$), which increases with increasing the cross-linking time before leveling off after 6 h.

The r values can be used to estimate the amount of functional groups and the V_w values, which yields the FFV values using Eq. (2). As shown in Table 1, the FFV value decreases with the cross-linking time before increasing, which is consistent with the changes of the density and T_g in the XLP84s. Interestingly, XLP84-6h has the lowest FFV value of 0.091.

Fig. 4 presents the thermal degradation behavior of P84 and XLP84-6h, which is very similar. Both polymers exhibit about 5 % mass loss at about 250 °C because of the loss of the residual NMP (with a boiling temperature of 203 °C), and then they are thermally stable at temperatures as high as 400 °C, indicating that they can be used for H₂/CO₂ separation at elevated temperatures such as 100 °C and 200 °C. The stability of the XLP84s cross-linked with BuDA is consistent with the P84 cross-linked with XDA [31]. On the other hand, the cross-linked Matrimid using ethylenediamine (EDA) were not stable at 100 °C or above [14, 15, 17], though the reaction mechanism of Matrimid and EDA is similar to that of P84 and BuDA investigated in this study. One of the possible reasons is that XLP84

was prepared with a cross-linking time of 1 h or more, while the literature study on Matrimid or 6FDA-durene often used 10 min or less and the cross-linking was confined to the surface. Another possibility can be the difference in the electrophilicity of imide rings among these polyimides. For example, Matrimid undergoes much more rapid cross-linking with PDA than 6FDA-durene because of the higher electron affinity in the dianhydride monomer used to synthesize Matrimid than that for 6FDA-durene [12]. However, it is beyond the scope of this study to fully elucidate the reaction mechanism of these polyimides with diamines.

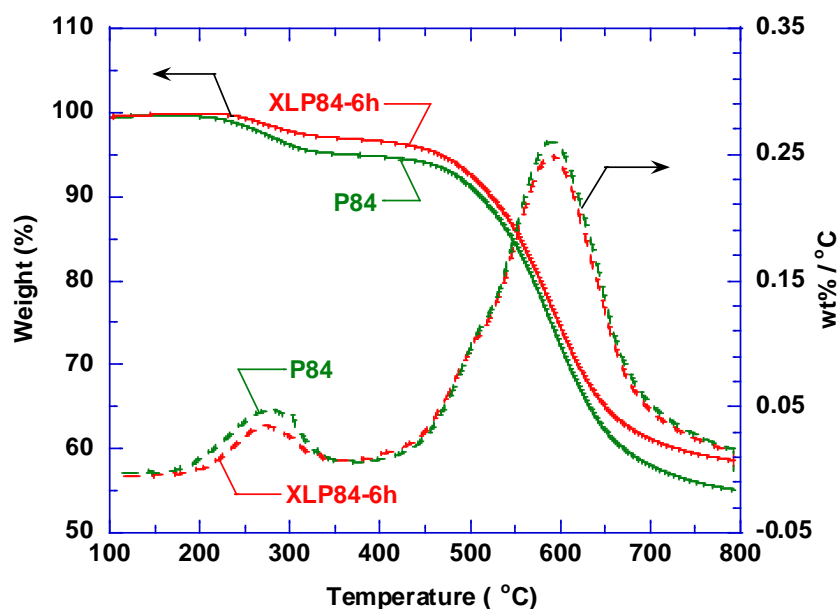


Fig. 4. Comparison of the thermal stability for P84 and XLP84-6h in the TGA (solid) and differential thermal gravimetric (DTG, dotted) curves.

3.2. Effect of cross-linking on gas permeability in XLP84s

The XLP84 samples were tested with pure-gas H₂ and CO₂ at pressures ranging from 4.4 atm to 11.2 atm and temperatures of 35 °C, 100 °C, and 150 °C, and the gas permeability is independent of the feed pressures. Fig. 5a and 5b present the effect of the cross-linking time on pure-gas H₂ and CO₂ permeability at 7.8 atm and various temperatures, respectively. As the cross-

linking time increases, H₂ permeability increases first before decreasing, and CO₂ permeability decreases consistently. As shown in Fig. 5c, the H₂/CO₂ selectivity increases from 5.8 to its maximum of 14 by 6 h cross-linking with a negligible decrease in H₂ permeability at 100 °C, validating that the cross-linking can improve the membrane H₂/CO₂ separation performance at high temperatures. The peak of the selectivity is also consistent with the chain relaxation of the P84 after 6 h sorption by methanol. Swelling time of more than 6 h appears to relax polymer chains and decrease the size-sieving ability. Polymer films were also tested at 100 °C and 150 °C continuously for more than 10 days while retaining their physical appearing and gas separation properties, indicating their thermal stability at the elevated temperatures, which is in contrast with Matrimid, 6FDA-durene, or 6FDA-ODA cross-linked with diamines [14, 15, 17, 26, 27].

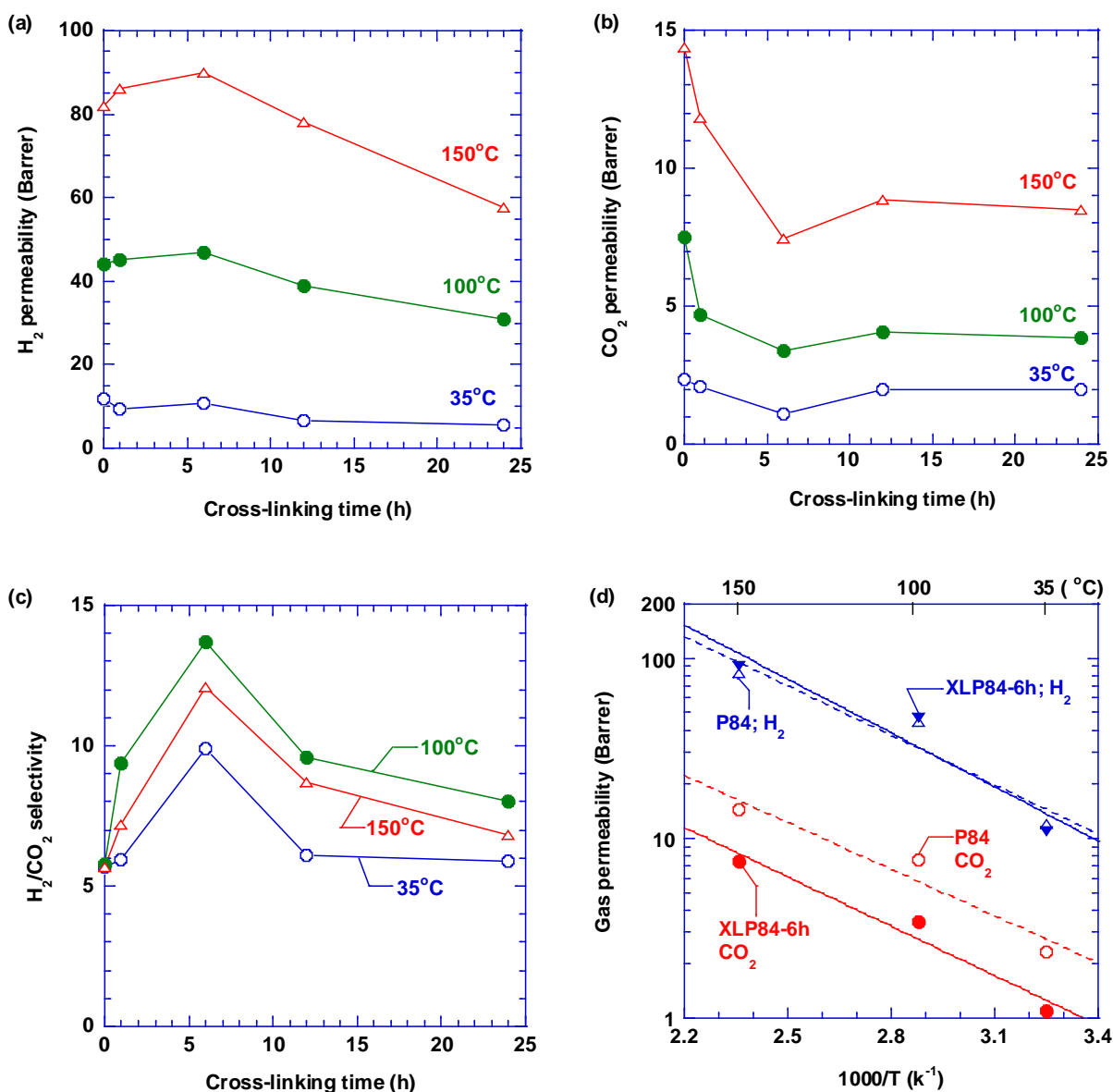


Fig. 5. Effect of the temperature and cross-linking time on (a) pure-gas H_2 permeability, (b) pure-gas CO_2 permeability, and (c) pure-gas H_2/CO_2 selectivity at 7.8 atm. (d) Modeling of pure-gas H_2 and CO_2 permeability in the P84 and XLP84-6h using the Arrhenius equation. Gas permeability has an estimated uncertainty of $\approx 10\%$, and the H_2/CO_2 selectivity has an uncertainty of $\approx 14\%$.

The effect of temperature on gas permeability can be described using the Arrhenius equation:

$$P_A = P_{A0} \exp\left(-\frac{E_{P,A}}{RT}\right) \quad (5)$$

where P_{A0} is a pre-exponential factor (Barrers), $E_{P,A}$ is the activation energy of permeation (kJ/mol), R is the gas constant, and T is the temperature (K). As shown in Fig. 5d, the gas permeability in the P84 and XLP84-6h can be satisfactorily described using the model. Table 2 records the adjustable parameters of $P_{A,0}$ and $E_{P,A}$ for H₂ and CO₂. For both samples, H₂ exhibits higher E_p values than CO₂, indicating a greater influence of the temperature on H₂ permeation than on CO₂ permeation. The XLP84-6h exhibits higher $E_{P,A}$ value for H₂ than P84, confirming the stronger size-sieving ability for XLP84-6h.

Table 2. Adjustable parameters of the Arrhenius equation for the gas permeability (at 7.8 atm), solubility (6.0 atm) and diffusivity in the pristine P84 and XLP84-6h at 35 - 150 °C.

Polymers	H ₂		CO ₂					
	P_{A0} (Barrer)	$E_{p,A}$ (kJ/mol)	P_{A0} (Barrer)	$E_{p,A}$ (kJ/mol)	S_{A0}^\dagger	$\Delta H_{S,A}$ (kJ/mol)	D_{A0} (10 ⁻⁴ cm ² /s)	$E_{D,A}$ (kJ/mol)
P84	24,000	18	1800	17	16	-14	8.7	31
XLP84-6h	13,600	19	1200	18	9.2	-16	9.9	34

[†] The unit is 10⁻³ cm³(STP)/(cm³ atm).

Fig. 6 compares the type of the diamines for 24-h cross-linking on the pure-gas H₂ permeability and H₂/CO₂ selectivity at 100 °C, including BuDA, XDA, and PDA. These diamines have different chain lengths and rigidity and have been widely explored for cross-linking Matrimid and 6FDA-durene. The BuDA cross-linked XLP84-24h exhibits the best combination of high H₂ permeability and H₂/CO₂ selectivity. The XDA cross-linked one shows comparable H₂/CO₂ selectivity but much lower H₂ permeability than the BuDA-crosslinked one, because the XDA with benzene ring interacts favorably with the benzene rings in P84 through π - π stacking, resulting in more compact structure and lower permeability than BuDA. The PDA cross-linked one shows both lower permeability and selectivity than the BuDA cross-linked one, presumably because of

the shorter and less flexible chains [12].

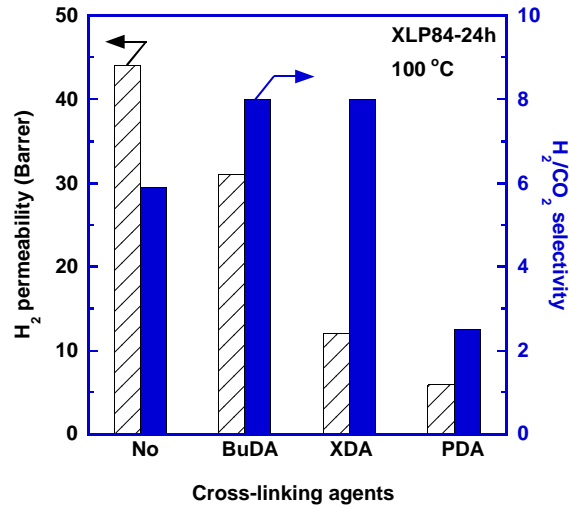


Fig. 6. Effect of the type of diamines on the pure-gas H₂ permeability and H₂/CO₂ selectivity at 100 °C. The cross-linking was performed for 24 h in methanol solutions. Gas permeability has an estimated uncertainty of ≈10%, and the H₂/CO₂ selectivity has an uncertainty of ≈14%.

3.3. Effect of cross-linking on gas solubility and diffusivity

To elucidate the effect of the cross-linking on the gas transport properties, gas permeability is decoupled into solubility and diffusivity. The CO₂ solubility was determined using a gravimetric method, while H₂ solubility could not be determined due to its extremely low sorption in polymers. Fig. 7a compares CO₂ sorption isotherms for P84 and XLP84-6h at different temperatures, showing that CO₂ sorption is independent of the cross-linking. The isotherms in glassy polymers can be described using the dual-mode sorption model:

$$C_A = k_D p_A + \frac{C'_H b p_A}{1 + b p_A} \quad (6)$$

where C_A is the sorption of the penetrant A in the polymer, k_D is the Henry's constant, C'_H is Langmuir sorption capacity, and b is the affinity parameter. Equation (6) also indicates that increasing gas pressure decreases solubility (S_A , where $S_A = C_A/p_A$). On the other hand, increasing

cross-linking time has minimal effect on the CO₂ solubility, as shown in Fig. 7b. The cross-linking does not drastically change the chemistry of the materials (indicated by less than 17 % of BuDA in the XLP84s, cf. Table 1). Because the gas solubility is governed by its condensability and interaction with the polymer matrix, the XLP84s show similar CO₂ solubility.

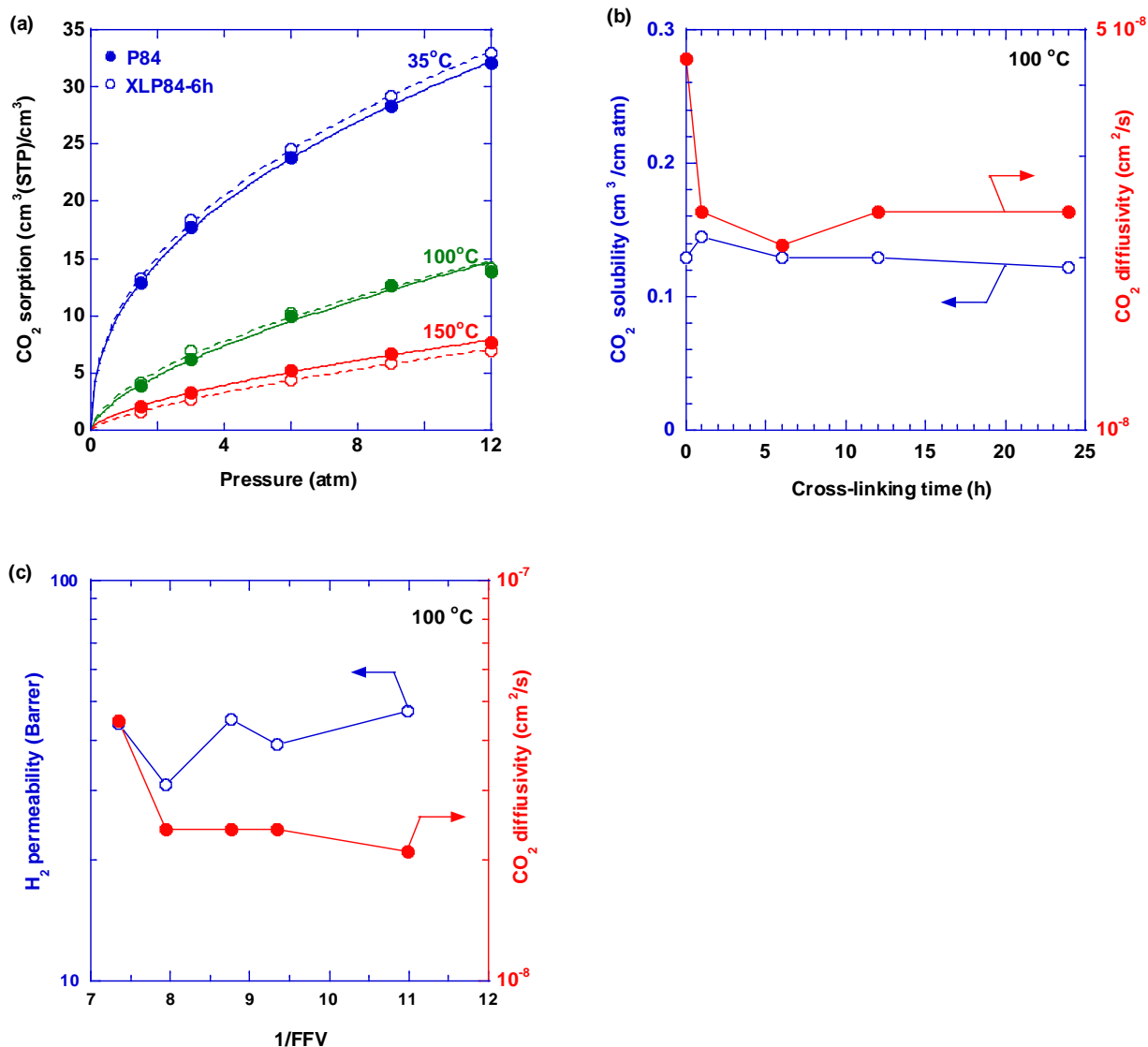


Fig. 7. (a) Effect of the temperature on the CO₂ sorption isotherms in P84 and XLP84-6h. (b) Effect of the cross-linking time on CO₂ solubility and diffusivity at 100 °C and 6 atm. (c) Effect of 1/FFV on H₂ permeability and CO₂ diffusivity at 100 °C. The CO₂ solubility and diffusivity have an estimated uncertainty of ≈5% and ≈11%, respectively.

Fig. 7b also shows that CO₂ diffusivity decreases significantly after 1 h cross-linking and then increases after 6 h cross-linking, which is consistent with the two-stage swelling kinetics. After 6 h swelling, the polymer chains relax, increasing the *FFV* for CO₂ diffusion. Fig. 7c illustrates that the decrease in the CO₂ diffusivity at 100 °C is consistent with the decrease in the *FFV*. However, there is no correlation between H₂ permeability and the polymer *FFV*, presumably because the distribution of the free volume size and population influence the gas permeability and such information cannot be directly determined.

The effect of the temperature on CO₂ solubility and diffusivity can also be described using the Arrhenius equations:

$$S_A = S_{A0} \exp\left(-\frac{\Delta H_{S,A}}{RT}\right) \quad (7)$$

$$D_A = D_{A0} \exp\left(-\frac{E_{D,A}}{RT}\right) \quad (8)$$

where S_{A0} (cm³(STP)/(cm³ atm)) and D_{A0} (cm²/s) are pre-exponential factors, $\Delta H_{S,A}$ is enthalpy of sorption (kJ/mol), and $E_{D,A}$ is the activation energy of diffusion (kJ/mol). The values of these parameters are summarized in Table 2. The $E_{D,A}$ value for CO₂ is slightly higher for XLP84-6h than the pristine P84, further confirming that cross-linking increases the size-sieving ability.

3.4. H₂/CO₂ separation properties in XLP84 at elevated temperatures

Fig. 8a compares the H₂/CO₂ separation properties in P84 and XLP84-6h with the materials reported in the literature at ≈35 °C in the Robeson's plot. The upper bound shows the tradeoff between H₂ permeability and H₂/CO₂ selectivity, and the 6 h cross-linking moves the performance of P84 closer to the upper bound at 35 °C, confirming the effectiveness of the cross-linking in improving the polymer separation properties. The upper bounds were also estimated for 100 °C and 150 °C using a transition state model developed in the literature [10, 40]. The pristine P84

shows the performance below the upper bounds for all the temperatures, while the XLP84-6h exhibits the H_2/CO_2 separation properties at the upper bound of 100 °C and close to that of 150 °C.

Fig. 8b displays the effect of the cross-linking time on the H_2/CO_2 separation properties at 100 °C. There appears to be an optimal cross-linking time (6 h), which yields the best combination of H_2 permeability and H_2/CO_2 selectivity right on the upper bound.

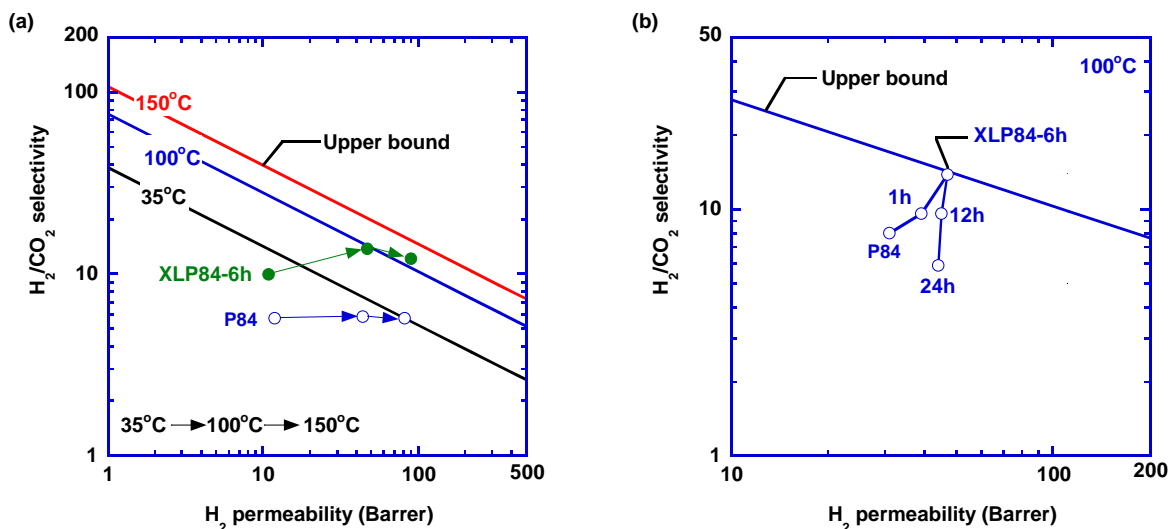


Fig. 8. (a) H_2/CO_2 separation performance of P84 and XLP84-6h in Robeson's upper bound plot at various temperatures. The data points from left to right are for 35 °C, 100 °C, and 150 °C, respectively. (b) Effect of the cross-linking time on the H_2/CO_2 separation performance at 100 °C.

4. Conclusions

Despite an extensive study of diamine-cross-linked polyimides for membrane H_2/CO_2 separation, this study, for the first time, systematically investigated the effect of the cross-linking of the bulk P84 films on H_2/CO_2 separation properties at elevated temperatures (> 100 °C). Unlike other polyimides such as Matrimid and 6FDA-durene, cross-linking P84 using BuDA decreases the sample mass while leading to highly cross-linked networks with thermal stability up to 400 °C. The XLP84 samples exhibit gas separation performance near the upper bound in Robeson's plot

for H₂/CO₂ separation at 100 °C to 150 °C, suggesting their potential for pre-combustion CO₂ capture.

Acknowledgments

This work was supported by the U.S. Department of Energy, Office of Fossil Energy, under Award Number DE-FE0026463. This work was also partially supported by the U.S. National Science Foundation (NSF) under the CAREER award number 1554236.

References

- [1] H. Kim, H. Yoon, S. Yoon, B. Yoo, B. Ahn, Y. Cho, H. Shin, H. Yang, U. Paik, S. Kwon, J. Choi, H. Park, Selective gas transport through few-layered graphene and graphene oxide membranes, *Science*, 342 (2013) 91-95.
- [2] H. Li, Z. Song, X. Zhang, Y. Huang, S. Li, Y. Mao, H. Ploehn, Y. Bao, M. Yu, Ultrathin, molecular-sieving graphene oxide membranes for selective hydrogen separation, *Science*, 342 (2013) 95-98.
- [3] L. Zhu, M.T. Swihart, H. Lin, Unprecedented size-sieving ability in polybenzimidazole doped with polyprotic acids for membrane H₂/CO₂ separation, *Energy Environ. Sci.*, 11 (2018) 94-100.
- [4] H. Lin, E. Van Wagner, B.D. Freeman, L.G. Toy, R.P. Gupta, Plasticization-enhanced H₂ purification using polymeric membranes, *Science*, 311 (2006) 639-642.
- [5] T.C. Merkel, M. Zhou, R.W. Baker, Carbon dioxide capture with membranes at an IGCC power plant, *J. Membr. Sci.*, 389 (2012) 441-450.
- [6] L. Shao, B. Low, T. Chung, A.R. Greenberg, Polymeric membranes for the hydrogen economy: Contemporary approaches and prospects for the future, *J. Membr. Sci.*, 327 (2009) 18-31.
- [7] K.A. Berchtold, R.P. Singh, J.S. Young, K.W. Dudeck, Polybenzimidazole composite membranes for high temperature synthesis gas separations, *J. Membr. Sci.*, 415-416 (2012) 265-270.
- [8] M. Galizia, W.S. Chi, Z.P. Smith, T.C. Merkel, R.W. Baker, B.D. Freeman, 50th anniversary perspective: Polymers and mixed matrix membranes for gas and vapor separation: A review and prospective opportunities, *Macromolecules*, 50 (2017) 7809-7843.
- [9] R.P. Singh, X. Li, K.W. Dudeck, B.C. Benicewicz, K.A. Berchtold, Polybenzimidazole based random copolymers containing hexafluoroisopropylidene functional groups for gas separations at elevated temperatures, *Polymer*, 119 (2017) 134-141.

- [10] L. Zhu, M.T. Swihart, H. Lin, Tightening polybenzimidazole (PBI) nanostructure via chemical cross-linking for membrane H₂/CO₂ separation, *J. Mater. Chem. A*, 5 (2017) 19914-19923.
- [11] Z. Ali, F. Pacheco, E. Litwiller, Y. Wang, Y. Han, I. Pinnau, Ultra-selective defect-free interfacially polymerized molecular sieve thin-film composite membranes for H₂ purification, *J. Mater. Chem. A*, 6 (2018) 30-35.
- [12] L. Shao, L. Liu, S. Cheng, Y. Huang, J. Ma, Comparison of diamino cross-linking in different polyimide solutions and membranes by precipitation observation and gas transport, *J. Membr. Sci.*, 312 (2008) 174-185.
- [13] P. Tin, T. Chung, Y. Liu, R. Wang, S. Liu, K.P. Pramoda, Effects of cross-linking modification on gas separation performance of Matrimid membranes, *J. Membr. Sci.*, 225 (2003) 77-90.
- [14] L. Shao, T. Chung, S. Goh, K. Pramoda, Polyimide modification by a linear aliphatic diamine to enhance transport performance and plasticization resistance, *J. Membr. Sci.*, 256 (2005) 46-56.
- [15] Y. Xiao, L. Shao, T. Chung, D.A. Schiraldi, Effects of thermal treatments and dendrimers chemical structures on the properties of highly surface cross-linked polyimide films, *Ind. Eng. Chem. Res.*, 44 (2005) 3059-3067.
- [16] T.S. Chung, L. Shao, P.S. Tin, Surface modification of polyimide membranes by diamines for H₂ and CO₂ separation, *Macromol. Rapid Commun.*, 27 (2006) 998-1003.
- [17] B. Low, Y. Xiao, T. Chung, Y. Liu, Simultaneous occurrence of chemical grafting, cross-linking, and etching on the surface of polyimide membranes and their impact on H₂/CO₂ separation, *Macromolecules*, 41 (2008) 1297-1309.
- [18] L. Shao, C.-H. Lau, T. Chung, A novel strategy for surface modification of polyimide membranes by vapor-phase ethylenediamine (EDA) for hydrogen purification, *Int. J. Hydrog. Energy*, 34 (2009) 8716-8722.
- [19] M. Chua, Y. Xiao, T. Chung, Using iron (III) acetylacetonate as both a cross-linker and micropore former to develop polyimide membranes with enhanced gas separation performance, *Sep. Purif. Techn.*, 133 (2014) 120-128.
- [20] H. Wang, T. Chung, D.R. Paul, Physical aging and plasticization of thick and thin films of the thermally rearranged ortho-functional polyimide 6FDA-HAB, *J. Membr. Sci.*, 458 (2014) 27-35.
- [21] S. Japip, K. Liao, T. Chung, Molecularly tuned free volume of vapor cross-linked 6FDA-durene/ZIF-71 MMMs for H₂/CO₂ separation at 150°C, *Adv. Mater.*, 29 (2017).
- [22] S.-H. Choi, J.C. Jansen, F. Tasselli, G. Barbieri, E. Drioli, In-line formation of chemically cross-linked P84[®] co-polyimide hollow fibre membranes for H₂/CO₂ separation, *Sep. Purif. Techn.*, 76 (2010) 132-139.
- [23] H. Wang, D.R. Paul, T. Chung, Surface modification of polyimide membranes by diethylenetriamine (DETA) vapor for H₂ purification and moisture effect on gas permeation, *J. Membr. Sci.*, 430 (2013) 223-233.
- [24] B. Low, Y. Xiao, T. Chung, Amplifying the molecular sieving capability of polyimide membranes via coupling of diamine networking and molecular architecture, *Polymer*, 50 (2009) 3250-3258.
- [25] C.H. Lau, B. Low, L. Shao, T. Chung, A vapor-phase surface modification method to enhance different types of hollow fiber membranes for industrial scale hydrogen separation, *Int. J. Hydrog. Energy*, 35 (2010) 8970-8982.

- [26] C.E. Powell, X.J. Duthie, S.E. Kentish, G.G. Qiao, G.W. Stevens, Reversible diamine cross-linking of polyimide membranes, *J. Membr. Sci.*, 291 (2007) 199-209.
- [27] L. Shao, T. Chung, S.H. Goh, K.P. Pramoda, The effects of 1,3-cyclohexanebis(methylamine) modification on gas transport and plasticization resistance of polyimide membranes, *J. Membr. Sci.*, 267 (2005) 78-89.
- [28] J. Campbell, J.D. Burgal, G. Szekely, R.P. Davies, D.C. Braddock, A. Livingston, Hybrid polymer/MOF membranes for Organic Solvent Nanofiltration (OSN): Chemical modification and the quest for perfection, *J. Membr. Sci.*, 503 (2016) 166-176.
- [29] Y.S. Toh, F. Lim, A. Livingston, Polymeric membranes for nanofiltration in polar aprotic solvents, *J. Membr. Sci.*, 301 (2007) 3-10.
- [30] M. Ungerank, G. Baumgarten, Polyimide membranes made of polymerization solutions, US Patent Application US20160310912A1, (2016).
- [31] X. Qiao, T. Chung, Diamine modification of P84 polyimide membranes for pervaporation dehydration of isopropanol, *AIChE J.*, 52 (2006) 3462-3472.
- [32] B. Lam, M. Wei, L. Zhu, S. Luo, R. Guo, A. Morisato, P. Alexandridis, H. Lin, Cellulose triacetate doped with ionic liquids for membrane gas separation, *Polymer*, 89 (2016) 1-11.
- [33] D.W. Van Krevelen, *Properties of Polymers: Their Correlation with Chemical Structure: Their Numerical Estimation and Prediction from Additive Group Contributions*, Elsevier, Amsterdam, 1990.
- [34] M. Yavari, T. Le, H. Lin, Physical aging of glassy perfluoropolymers in thin film composite membranes. Part I. Gas transport properties, *J. Membr. Sci.*, 525 (2017) 387-398.
- [35] P.R. Bevington, D.K. Robinson, *Data Reduction and Error Analysis for the Physical Sciences*, 2nd ed., McGraw-Hill, Inc., New York, 1992.
- [36] S.N. Dhoot, B.D. Freeman, M.E. Stewart, A.J. Hill, Sorption and transport of linear alkane hydrocarbons in biaxially oriented polyethylene terephthalate, *J. Polym. Sci. B: Polym. Phys.*, 39 (2001) 1160-1172.
- [37] D.W. Mangindaan, G. Shi, T. Chung, Pervaporation dehydration of acetone using P84 copolyimide flat sheet membranes modified by vapor phase crosslinking, *J. Membr. Sci.*, 458 (2014) 76-85.
- [38] H. Eguchi, D.J. Kim, W.J. Koros, Chemically cross-linkable polyimide membranes for improved transport plasticization resistance for natural gas separation, *Polymer*, 58 (2015) 121-129.
- [39] L. Zhu, M. Omidvar, H. Lin, Manipulating Polyimide Nanostructures via Cross-linking for Membrane Gas Separation, in: M.A. Carreon (Ed.) *Membranes for Gas Separations*, World Scientific Publishing Co., Hackensack, NJ, 2017, pp. 243-267.
- [40] B.W. Rowe, L.M. Robeson, B.D. Freeman, D.R. Paul, Influence of temperature on the upper bound: Theoretical considerations and comparison with experimental results, *J. Membr. Sci.*, 360 (2010) 58-69.